Chapter 1

Motivation: Mechanics and Optics

A mathematical billiard consists of a domain, say, in the plane (a billiard table), and a point-mass (a billiard ball) that moves inside the domain freely. This means that the point moves along a straight line with a constant speed until it hits the boundary. The reflection off the boundary is elastic and subject to a familiar law: *the angle of incidence equals the angle of reflection*. After the reflection, the point continues its free motion with the new velocity until it hits the boundary again, etc.; see figure 1.1.

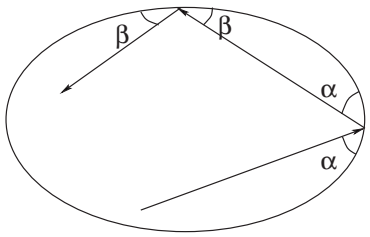

Figure 1.1. Billiard reflection

An equivalent description of the billiard reflection is that, at the impact point, the velocity of the incoming billiard ball is decomposed

into the normal and tangential components. Upon reflection, the normal component instantaneously changes sign, while the tangential one remains the same. In particular, the speed of the point does not change, and one may assume that the point always moves with the unit speed.

This description of the billiard reflection applies to domains in multi-dimensional space and, more generally, to other geometries, not only to the Euclidean one. Of course, we assume that the reflection occurs at a smooth point of the boundary. For example, if the billiard ball hits a corner of the billiard table, the reflection is not defined and the motion of the ball terminates right there.

There are many questions one asks about the billiard system; many of them will be discussed in detail in these notes. As a sample, let D be a plane billiard table with a smooth boundary. We are interested in 2-periodic, back and forth, billiard trajectories inside D. In other words, a 2-periodic billiard orbit is a segment inscribed in D which is perpendicular to the boundary at both end points. The following exercise is rather hard; the reader will have to wait until Chapter 6 for a relevant discussion.

Exercise 1.1. a) Does there exist a domain D without a 2-periodic billiard trajectory?

b) Assume that D is also convex. Show that there exist at least two distinct 2-periodic billiard orbits in D.

c) Let D be a convex domain with smooth boundary in three-dimensional space. Find the least number of 2-periodic billiard orbits in D.

d) A disc D in the plane contains a one parameter family of 2-periodic billiard trajectories making a complete turn inside D (these trajectories are the diameters of D). Are there other plane convex billiard tables with this property?

In this chapter, we discuss two motivations for the study of mathematical billiards: from classical mechanics of elastic particles and from geometrical optics.

Example 1.2. Consider the mechanical system consisting of two point-masses m_1 and m_2 on the positive half-line $x \geq 0$. The collision

between the points is elastic; that is, the energy and momentum are conserved. The reflection off the left end point of the half-line is also elastic: if a point hits the "wall" $x = 0$, its velocity changes sign.

Let x_1 and x_2 be the coordinates of the points. Then the state of the system is described by a point in the plane (x_1, x_2) satisfying the inequalities $0 \le x_1 \le x_2$. Thus the *configuration space* of the system is a plane wedge with the angle $\pi/4$.

Let v_1 and v_2 be the speeds of the points. As long as the points do not collide, the phase point (x_1, x_2) moves with constant speed (v_1, v_2). Consider the instance of collision, and let u_1, u_2 be the speeds after the collision. The conservation of momentum and energy reads as follows:

$$(1.1)\quad m_1u_1 + m_2u_2 = m_1v_1 + m_2v_2, \frac{m_1u_1^2}{2} + \frac{m_2u_2^2}{2} = \frac{m_1v_1^2}{2} + \frac{m_2v_2^2}{2}.$$

Introduce new variables: $\bar{x}_i = \sqrt{m_i}x_i;\ i = 1, 2$. In these variables, the configuration space is the wedge whose lower boundary is the line $\bar{x}_1/\sqrt{m_1} = \bar{x}_2/\sqrt{m_2}$; the angle measure of this wedge is equal to $\arctan\sqrt{m_1/m_2}$ (see figure 1.2).

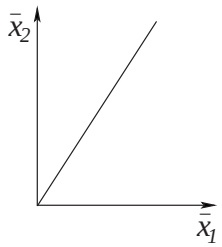

Figure 1.2. Configuration space of two point-masses on the half-line

In the new coordinate system, the speeds rescale the same way as the coordinates: $\bar{v}_1 = \sqrt{m_1}v_1$, etc. Rewriting (1.1) yields:

$$(1.2)\quad \sqrt{m_1}\ \bar{u}_1 + \sqrt{m_2}\ \bar{u}_2 = \sqrt{m_1}\ \bar{v}_1 + \sqrt{m_2}\ \bar{v}_2, \quad \bar{u}_1^2 + \bar{u}_2^2 = \bar{v}_1^2 + \bar{v}_2^2.$$

The second of these equations means that the magnitude of the velocity vector $(\bar{v}_1, \bar{v}_2)$ does not change in the collision. The first equation in (1.2) means that the dot product of the velocity vector with the

vector $(\sqrt{m_1}, \sqrt{m_2})$ is preserved as well. The latter vector is tangent to the boundary line of the configuration space: $\bar{x}_1/\sqrt{m_1} = \bar{x}_2/\sqrt{m_2}$. Hence the tangential component of the velocity vector does not change, and the configuration trajectory reflects in this line according to the billiard law.

Likewise one considers a collision of the left point with the wall $x = 0$; such a collision corresponds to the billiard reflection in the vertical boundary component of the configuration space. We conclude that the system of two elastic point-masses m_1 and m_2 on the half-line is isomorphic to the billiard in the angle $\arctan\sqrt{m_1/m_2}$.

As an immediate corollary, we can estimate the number of collisions in our system. Consider the billiard system inside an angle α. Instead of reflecting the billiard trajectory in the sides of the wedge, reflect the wedge in the respective side and unfold the billiard trajectory to a straight line; see figure 1.3. This *unfolding*, suggested by geometrical optics, is a very useful trick when studying billiards inside polygons.

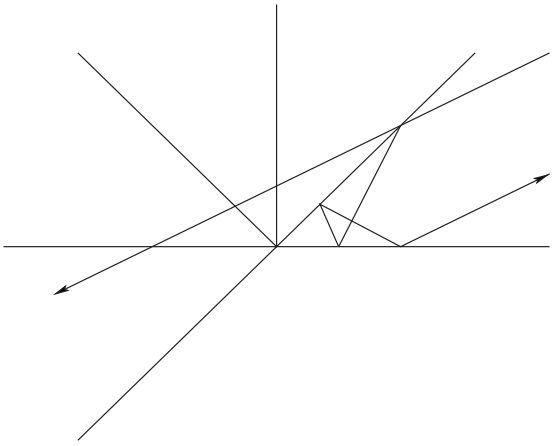

Figure 1.3. Unfolding a billiard trajectory in a wedge

Unfolding a billiard trajectory inside a wedge, we see that the number of reflections is bounded above by $\lceil \pi/\alpha \rceil$ (where $\lceil x \rceil$ is the ceiling function, the smallest integer not less than x). For the system

of two point-masses on the half-line, the upper bound for the number of collisions is

$$\left\lceil \frac{\pi}{\arctan\sqrt{m_1/m_2}} \right\rceil. \tag{1.3}$$

Exercise 1.3. Extend the upper bound on the number of collisions to a wedge convex inside; see figure 1.4.

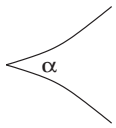

Figure 1.4. A plane wedge, convex inside

Exercise 1.4. a) Interpret the system of two point-masses on a segment, subject to elastic collisions with each other and with the end points of the segment, as a billiard.

b) Show that the system of three point-masses m_1, m_2, m_3 on the line, subject to elastic collisions with each other, is isomorphic to the billiard inside a wedge in three-dimensional space. Prove that the dihedral angle of this wedge is equal to

$$\arctan\left(m_2\sqrt{\frac{m_1+m_2+m_3}{m_1m_2m_3}}\right). \tag{1.4}$$

c) Choose the system of reference at the center of mass and reduce the above system to the billiard inside a plane angle (1.4).

d) Investigate the system of three elastic point-masses on the half-line.

1.1. Digression. Billiard computes π. Formula (1.3) makes it possible to compute the first decimal digits of π. What follows is a brief account of G. Galperin's article [**39**].

Consider two point-masses on the half-line and assume that $m_2 = 100^k m_1$. Let the first point be at rest and give the second a push to the left. Denote by $N(k)$ the total number of collisions and reflections in this system, finite by the above discussion. The claim is that

$$N(k) = 31415926535897932384626433 83\ldots,$$

the number made of the first $k+1$ digits of π. Let us explain why this claim almost certainly holds.

With the chosen initial data (the first point at rest), the configuration trajectory enters the wedge in the direction, parallel to the vertical side. In this case, the number of reflections is given by a modification of formula (1.3), namely

$$N(k) = \left\lceil \frac{\pi}{\arctan\left(10^{-k}\right)} \right\rceil - 1.$$

This fact is established by the same unfolding method.

For now, denote 10^{-k} by x. This x is a very small number, and one expects $\arctan x$ to be very close to x. More precisely,

$$0 < \left(\frac{1}{\arctan x} - \frac{1}{x} \right) < x \quad \text{for } x > 0. \tag{1.5}$$

Exercise 1.5. Prove (1.5) using the Taylor expansion for $\arctan x$.

The first k digits of the number

$$\left\lceil \frac{\pi}{x} \right\rceil - 1 = \lceil 10^k \pi \rceil - 1 = \lfloor 10^k \pi \rfloor$$

coincide with the first $k+1$ decimal digits of π. The second equality follows from the fact that $10^k\pi$ is not an integer; $\lfloor y \rfloor$ is the floor function, the greatest integer not greater than y.

We will be done if we show that

$$\left\lceil \frac{\pi}{x} \right\rceil = \left\lceil \frac{\pi}{\arctan x} \right\rceil. \tag{1.6}$$

By (1.5),

$$\left\lceil \frac{\pi}{x} \right\rceil \le \left\lceil \frac{\pi}{\arctan x} \right\rceil \le \left\lceil \frac{\pi}{x} + \pi x \right\rceil. \tag{1.7}$$

The number $\pi x = 0.0\ldots031415\ldots$ has $k-1$ zeros after the decimal dot. Therefore the left- and the right-hand sides in (1.7) can differ only if there is a string of $k-1$ nines following the first $k+1$ digits in the decimal expansion of π. We do not know whether such a string ever occurs, but this is extremely unlikely for large values of k. If one does not have such a string, then both inequalities in (1.7) are equalities, (1.6) holds, and the claim follows. ♣

Let us proceed with examples of mechanical systems leading to billiards. Example 1.2 is quite old, and I do not know where it was considered for the first time. The next example, although similar to the previous one, is surprisingly recent; see [**45, 29**].

Example 1.6. Consider three elastic point-masses m_1, m_2, m_3 on the circle. We expect this mechanical system also to be isomorphic to a billiard.

Let x_1, x_2, x_3 be the angular coordinates of the points. Considering S^1 as $\mathbf{R}/2\pi\mathbf{Z}$, lift the coordinates to real numbers and denote the lifted coordinates by the same letters with bar (this lift is not unique: one may change each coordinate by a multiple of 2π). Rescale the coordinates as in Example 1.2. Collisions between pairs of points correspond to three families of parallel planes in three-dimensional space:

$$\frac{\bar{x}_1}{\sqrt{m_1}} = \frac{\bar{x}_2}{\sqrt{m_2}} + 2\pi k, \frac{\bar{x}_2}{\sqrt{m_2}} = \frac{\bar{x}_3}{\sqrt{m_3}} + 2\pi m, \frac{\bar{x}_3}{\sqrt{m_3}} = \frac{\bar{x}_1}{\sqrt{m_1}} + 2\pi n$$

where $k, m, n \in \mathbf{Z}$.

All the planes involved are orthogonal to the plane

$$\sqrt{m_1}\bar{x}_1 + \sqrt{m_2}\bar{x}_2 + \sqrt{m_3}\bar{x}_3 = const, \tag{1.8}$$

and they partition this plane into congruent triangles. The planes partition space into congruent infinite triangular prisms, and the system of three point-masses on the circle is isomorphic to the billiard inside such a prism. The dihedral angles of the prisms were already computed in Exercise 1.4 b).

Arguing as in Exercise 1.4 c), one may reduce one degree of freedom. Namely, the center of mass of the system has the angular speed

$$\frac{m_1v_1 + m_2v_2 + m_3v_3}{m_1 + m_2 + m_3}.$$

One may choose the system of reference at this center of mass which, in the new coordinates, means that

$$\sqrt{m_1}\bar{v}_1 + \sqrt{m_2}\bar{v}_2 + \sqrt{m_3}\bar{v}_3 = 0,$$

and therefore equation (1.8) holds. In other words, our system reduces to the billiard inside an acute triangle with the angles

$$\arctan\left(m_i\sqrt{\frac{m_1+m_2+m_3}{m_1m_2m_3}}\right), \quad i=1,2,3.$$

Remark 1.7. Exercise 1.4 and Example 1.6 provide mechanical systems, isomorphic to the billiards inside a right or an acute triangle. It would be interesting to find a similar interpretation for an obtuse triangle.

Exercise 1.8. This problem was communicated by S. Wagon. Suppose 100 identical elastic point-masses are located somewhere on a one-meter interval and each has a certain speed, not less than 1 m/s, either to the left or the right. When a point reaches either end of the interval, it falls off and disappears. What is the longest possible waiting time until all points are gone?

In dimensions higher than 1, it does not make sense to consider point-masses: with probability 1, they will never collide. Instead one considers the system of hard balls in a vessel; the balls collide with the walls and with each other elastically. Such a system is of great interest in statistical mechanics: it serves a model of ideal gas.

In the next example, we will consider one particular system of this type. Let us first describe collision between two elastic balls. Let two balls have masses m_1, m_2 and velocities v_1, v_2 (we do not specify the dimension of the ambient space). Consider the instance of collision. The velocities are decomposed into the radial and the tangential components:

$$v_i = v_i^r + v_i^t, \quad i=1,2,$$

the former having the direction of the axis connecting the centers of the balls, and the latter perpendicular to this axis. In collision, the tangential components remain the same, and the radial components change as if the balls were colliding point-masses in the line, that is, as in (1.1).

Exercise 1.9. Consider a non-central collision of two identical elastic balls. Prove that if one ball was at rest, then after the collision the balls will move in orthogonal directions.

Example 1.10. Consider the system of two identical elastic discs of radius r on the "unit" torus $\mathbf{R}^2/\mathbf{Z}^2$. The position of a disc is characterized by its center, a point on the torus. If x_1 and x_2 are the positions of the two centers, then the distance between x_1 and x_2 is not less than $2r$. The set of such pairs (x_1, x_2) is the configuration space of our system. Each x_i can be lifted to $\mathbf{R}^2$; such a lift is defined up to addition of an integer vector. However, the velocity v_i is a well defined vector in $\mathbf{R}^2$.

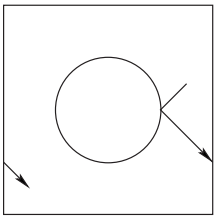

Figure 1.5. Reduced configuration space of two discs on the torus

Similarly to Example 1.6, one can reduce the number of degrees of freedom by fixing the center of mass of the system. This means that we consider the difference $x = x_2 - x_1$ which is a point of the torus at distance at least $2r$ from the point representing the origin in $\mathbf{R}^2$; see figure 1.5. Thus the reduced configuration space is the torus with a hole, a disc of radius $2r$. The velocity of this configuration point is the vector $v_2 - v_1$.

When the two discs collide, the configuration point is on the boundary of the hole. Let v be the velocity of point x before the collision and u after it. Then we have decompositions

$$v = v_2 - v_1 = (v_2^t - v_1^t) + (v_2^r - v_1^r), \quad u = u_2 - u_1 = (u_2^t - u_1^t) + (u_2^r - u_1^r).$$

The law of reflection implies that the tangential components do not change: $u_1^t = v_1^t, u_2^t = v_2^t$. To find u_1^r and u_2^r, use (1.1) with $m_1 = m_2$. The solution of this system is: $u_1^r = v_2^r, u_2^r = v_1^r$. Hence $u = (v_2^t - v_1^t) - (v_2^r - v_1^r)$. Note that the vector $v_2^t - v_1^t$ is perpendicular to x and thus tangent to the boundary of the configuration space, while the vector $v_2^r - v_1^r$ is collinear with x and hence normal to the boundary.

Therefore the vector u is obtained from v by the billiard reflection off the boundary.

We conclude that the (reduced) system of two identical elastic discs on the torus is isomorphic to the billiard on the torus with a disc removed. This billiard system is known as the Sinai billiard, [**100, 101**]. This was the first example of a billiard system that exhibits a chaotic behavior; we will talk about such billiards in Chapter 8.

Examples 1.2, 1.6 and 1.10 confirm a general principle: a conservative mechanical system with elastic collisions is isomorphic to a certain billiard.

1.2. Digression. Configuration spaces. Introduction of configuration space is a conceptually important and non-trivial step in the study of complex systems. The following instructive example is common in the Russian mathematical folklore; it is due to N. Konstantinov (cf. [**4**]).

Consider the next problem. Towns A and B are connected by two roads. Suppose that two cars, connected by a rope of length $2r$, can go from A to B without breaking the rope. Prove that two circular wagons of radius r moving along these roads in the opposite directions will necessarily collide.

To solve the problem, parameterize each road from A to B by the unit segment. Then the configuration space of pairs of points, one on each road, is the unit square. The motion of the cars from A to B is represented by a continuous curve connecting the points $(0,0)$ and $(1,1)$. The motion of the wagons is represented by a curve connecting the points $(0,1)$ and $(1,0)$. These curves must intersect, and an intersection point corresponds to collision of the wagons; see figure 1.6.

An interesting class of configuration spaces is provided by plane linkages, systems of rigid rods with hinge connections. For example, a pendulum is one rod, fixed at its end point; its configuration space is the circle S^1. A double pendulum consists of two rods, fixed at one end point; its configuration space is the torus $T^2 = S^1 \times S^1$.

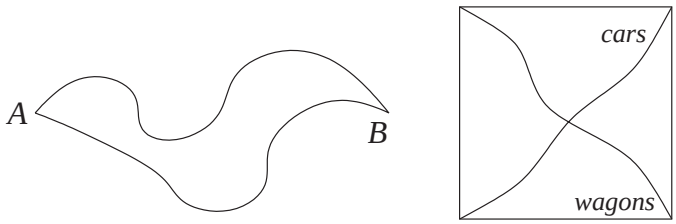

Figure 1.6. The two roads problem

Exercise 1.11. Consider a linkage made of four unit segments connecting fixed points located at distance $d \leq 4$; see figure 1.7.

a) Find the dimension of the configuration space of this linkage.

b) Let $d = 3.9$. Prove that the configuration space is the sphere S^2.

c)* Let $d = 1$. Prove that the configuration space is the sphere with four handles, that is, a surface of genus 4.

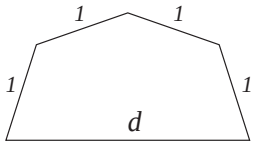

Figure 1.7. A plane linkage

This exercise has convinced you that, although a plane linkage is a very simple mechanism, its configuration space may have a complicated topology. In fact, this topology can be arbitrarily complicated (we do not discuss the exact meaning of this statement; see [**56**]).

To conclude this digression, let us mention a very simple system: a line in space, fixed at the origin. The configuration space is $\mathbf{RP}^2$, the real projective plane; see Digression 5.4 for a discussion. If the line is considered in $\mathbf{R}^n$, then the configuration space is the real projective space $\mathbf{RP}^{n-1}$. This space plays a very prominent role in geometry and topology. Of course, if the line is oriented, then the respective configuration space is the sphere S^{n-1}. ♣

Now let us briefly discuss another source of motivation for the study of billiards, geometrical optics. According to the *Fermat principle*, light propagates from point A to point B in the least possible time. In a homogeneous and isotropic medium, that is, in Euclidean geometry, this means that light "chooses" the straight line AB.

Consider now a single reflection in a mirror that we assume to be a straight line l in the plane; see figure 1.8. Now we are looking for a broken line AXB of minimal length where $X \in l$. To find the position of point X, reflect point B in the mirror and connect to A. Clearly, for any other position of point X, the broken line $AX'B$ is longer than AXB. This construction implies that the angles made by the incoming and outgoing rays AX and XB with the mirror l are equal. We obtain the billiard reflection law as a consequence of the Fermat principle.

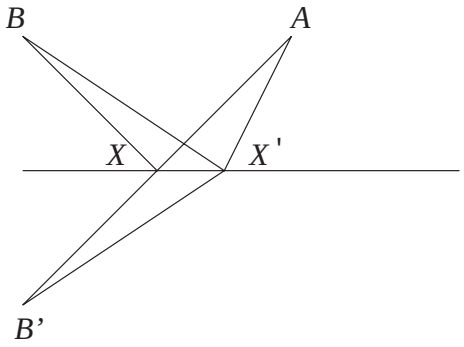

Figure 1.8. Reflection in a flat mirror

Exercise 1.12. Let A and B be points inside a plane wedge. Construct a ray of light from A to B reflecting in each side of the wedge.

Let the mirror be an arbitrary smooth curve l; see figure 1.9. The variational principle still applies: the reflection point X extremizes the length of the broken line AXB. Let us use calculus to deduce the reflection law. Let X be a point of the plane, and define the function $f(X) = |AX| + |BX|$. The gradient of the function $|AX|$ is the unit vector in the direction from A to X, and likewise for $|BX|$. We are

interested in critical points of $f(X)$, subject to the constraint $X \in l$. By the Lagrange multipliers principle, X is a critical point if and only if $\nabla f(X)$ is orthogonal to l. The sum of the unit vectors from A to X and from B to X is perpendicular to l if and only if AX and BX make equal angles with l. We have again obtained the billiard reflection law. Of course, the same argument works if the mirror is a smooth hypersurface in multi-dimensional space, and in Riemannian geometries other than Euclidean.

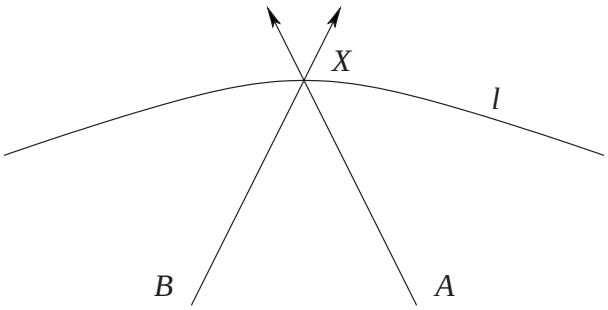

Figure 1.9. Reflection in a curved mirror

The above argument could be rephrased using a different mechanical model. Let l be wire, X a small ring that can move along the wire without friction, and AXB an elastic string fixed at points A and B. The string assumes minimal length, and the equilibrium condition for the ring X is that the sum of the two equal tension forces along the segments XA and XB is orthogonal to l. This implies the equal angles condition.

1.3. Digression. Huygens principle, Finsler metric, Finsler billiards. The speed of light in a non-homogeneous anisotropic medium depends on the point and the direction. Then the trajectories of light are not necessarily straight lines. A familiar example is a ray of light going from air to water; see figure 1.10. Let c_1 and c_0 be the speeds of light in water and in air. Then $c_1 < c_0$, and the trajectory of light is a broken line satisfying *Snell's law*

$$\frac{\cos\alpha}{\cos\beta} = \frac{c_0}{c_1}.$$

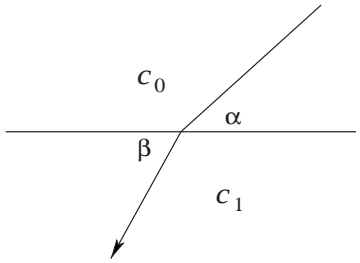

Figure 1.10. Snell's law

Exercise 1.13. Deduce Snell's law from the Fermat principle.[1]

To describe optical properties of the medium, one defines the "unit sphere" $S(X)$ at every point X: it consists of the unit tangent vectors at X. The hypersurface S is called *indicatrix*; we assume it is smooth, centrally symmetric and strictly convex. For example, in the case of Euclidean space, the indicatrices at all points are the same unit spheres. A field of indicatrices determines the so-called *Finsler metric*: the distance between points A and B is the least time it takes light to get from A to B. A particular case of Finsler geometry is the Riemannian one. In the latter case, one has a (variable) Euclidean structure in the tangent space at every point X, and the indicatrix $S(X)$ is the unit sphere in this Euclidean structure.

Another example is a *Minkowski metric*. This is a Finsler metric in a vector space whose indicatrices at different points are obtained from each other by parallel translations. The speed of light in a Minkowski space depends on the direction but not the point; this is a homogeneous but anisotropic medium. Minkowski's motivation for the study of these geometries came from number theory.

Propagation of light satisfies the *Huygens principle*. Fix a point A and consider the locus of points F_t reached by light in a fixed time t. The hypersurface F_t is called a wave front, and it consists of the points at Finsler distance t from A. The Huygens principle states that the front $F_{t+\varepsilon}$ can be constructed as follows: every point of F_t is

[1]There was a heated polemic between Fermat and Descartes concerning whether the speed of light increases or decreases with the density of the medium. Descartes erroneously thought that light moves faster in water than in the air.

considered a source of light, and $F_{t+\varepsilon}$ is the envelope of the ε-fronts of these points. Let $X \in F_t$ and let u be the Finsler unit tangent vector to the trajectory of light from A to X. An infinitesimal version of the Huygens principle states that the tangent space to the front $T_X F_t$ is parallel to the tangent space to the indicatrix $T_u S(X)$ at point u; see figure 1.11.

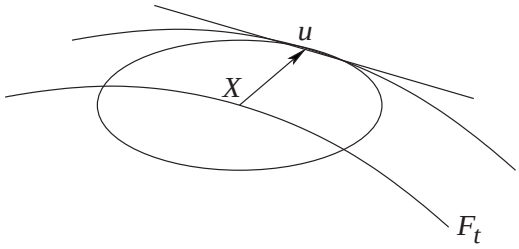

Figure 1.11. Huygens principle

We are in a position to deduce the billiard reflection law in Finsler geometry. To fix ideas, let us consider the two-dimensional situation. Let l be a smooth curved mirror (or the boundary of a billiard table) and AXB the trajectory of light from A to B. As usual, we assume that point X extremizes the Finsler length of the broken line AXB.

Theorem 1.14. *Let u and v be the Finsler unit vectors tangent to the incoming and outgoing rays. Then the tangent lines to the indicatrix $S(X)$ at points u and v intersect at a point on the tangent line to l at X; see figure 1.12 featuring the tangent space at point X.*

Proof. We repeat, with appropriate modifications, the argument in the Euclidean case. Consider the functions $f(X) = |AX|$ and $g(X) = |BX|$ where the distances are understood in the Finsler sense. Let ξ and η be tangent vectors to the indicatrix $S(X)$ at points u and v. One has, for the directional derivative, $D_u(f) = 1$ since u is tangent to the trajectory of light from A to X. On the other hand, by the Huygens principle, ξ is tangent to the front of point A that passes through point X. This front is a level curve of the function f; hence $D_\xi(f) = 0$. Likewise, $D_\eta(g) = 0$ and $D_v(g) = -1$.

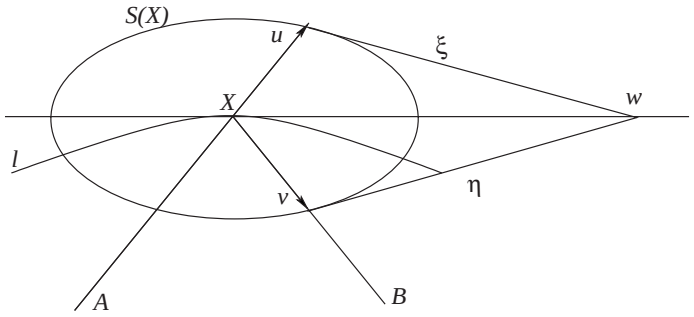

Figure 1.12. Finsler billiard reflection

Let w be the intersection point of the tangent lines to $S(X)$ at points u and v. Then $w = u + a\xi = v + b\eta$ where a, b are some reals. It follows that $D_w(f) = 1, D_w(g) = -1$ and $D_w(f + g) = 0$. If w is tangent to the mirror l, then X is a critical point of the function $f + g$, Finsler length of the broken line AXB. This establishes the Finsler reflection law. □

Of course, if the indicatrix is a circle, one obtains the familiar law of equal angles. For more information on propagation of light and Finsler geometry, in particular, Finsler billiards, see [**2, 3, 8, 49**]. ♣

1.4. Digression. Brachistochrone. One of the most famous problems in mathematical analysis concerns the trajectory of a mass point going from one point to another in least time, subject to the gravitational force. This curve is called brachistochrone (in Greek, "shortest time"). The problem was posed by Johann Bernoulli at the end of the 17th century and solved by him, his brother Jacob, Leibnitz, L'Hospital and Newton. In this digression we describe the solution of Johann Bernoulli who approached the problem from the point of view of geometrical optics; see, e.g., [**44**] for a historical panorama.

Let A and B be the starting and terminal points of the desired curve, and let x be the horizontal and y the vertical axes. It is convenient to direct the y axis downward and assume that the y-coordinate of A is zero. Suppose that a point-mass dropped a vertical distance y. Then its potential energy reduces by mgy where g is the

gravitational constant and m is the mass. Let $v(y)$ be the speed of the point-mass. Its kinetic energy equals $mv(y)^2/2$, and it follows from conservation of energy that

$$v(y) = \sqrt{2gy}. \tag{1.9}$$

Thus the speed of the point-mass depends only on its vertical coordinate.

Consider the medium described by equation (1.9). According to the Fermat principle, the desired curve is the trajectory of light from A to B. One can approximate the continuous medium by a discrete one consisting of thin horizontal strips in which the speed of light is constant. Let $v_1, v_2, \dots$ be the speeds of light in the first, second, etc., strips, and let $\alpha_1, \alpha_2, \dots$ be the angles made by the trajectory of light (a polygonal line) with the horizontal border lines between consecutive strips. By Snell's law, $\cos\alpha_i/v_i = \cos\alpha_{i+1}/v_{i+1}$; see figure 1.10. Thus, for all i,

$$\frac{\cos\alpha_i}{v_i} = const. \tag{1.10}$$

Now return to the continuous case. Taking (1.9) into account, equation (1.10) yields, in the continuous limit:

$$\frac{\cos\alpha(y)}{\sqrt{y}} = const. \tag{1.11}$$

Taking into account that $\tan\alpha = dy/dx$, equation (1.11) gives a differential equation for the brachistochrone $y' = \sqrt{(C-y)/y}$; this equation can be solved, and Johann Bernoulli knew the answer: its solution is the cycloid, the trajectory of a point on a circle that rolls, without sliding, along a horizontal line; see figure 1.13.[2]

In fact, the argument proving equation (1.11) gives much more. One does not have to assume that the speed of light depends on y only. Assume, more generally, that the speed of light at point (x, y) is given by a function $v(x, y)$ (so it does not depend on the direction, and the medium is anisotropic). Consider the level curves of the function v and let γ be a trajectory of light in this medium. Let t be the speed of light along γ considered as a function on this curve. Denote by

[2]Incidentally, the cycloid also solves another problem: to find a curve AB such that a mass point, sliding down the curve, arrives at the end point B in the same time, no matter where on the curve it started.

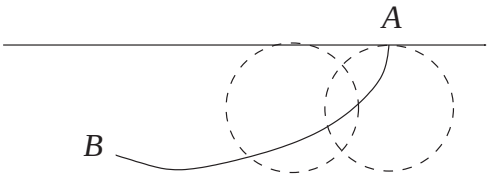

Figure 1.13. Brachistochrone

$\alpha(t)$ the angle between γ and the respective level curve $v(x, y) = t$. A generalization of equation (1.11) is given by the following theorem.

Theorem 1.15. *Along a trajectory γ, one has:*

$$\frac{\cos \alpha(t)}{t} = const.$$

Exercise 1.16. a) Let the speed of light be given by the function $v(x, y) = y$. Prove that the trajectories of light are arcs of circles centered on the line $y = 0$.

b) Let the speed of light be given by the function $v(x, y) = 1/\sqrt{c - y}$. Prove that the trajectories of light are arcs of parabolas.

c) Let the speed of light be $v(x, y) = \sqrt{1 - x^2 - y^2}$. Prove that the trajectories of light are arcs of circles perpendicular to the unit circle centered at the origin. ♣

To conclude this chapter, let us mention numerous variations of the billiard set-up. For example, one may consider billiards in potential fields. Another interesting modification, popular in the physical literature, is the billiard in a magnetic field; see [**16, 115**]. The strength of a magnetic field, perpendicular to the plane, is given by a function on the plane B. A charge at point x is acted upon by the *Lorentz force*, proportional to $B(x)$ and to its speed v; the Lorentz force acts in the direction perpendicular to the motion. The free path of such a point-charge is a curve whose curvature at every point is prescribed by the function B. For example, if the magnetic field is constant, then the trajectories are circles of the *Larmor radius*

v/B.[3] When the point-charge hits the boundary of the billiard table, it reflects elastically, so the magnetic field does not affect the reflection law. A peculiar feature of magnetic billiards is their time-irreversibility: if one changes the velocity to the opposite, the point-charge will not traverse its trajectory backward (unless the magnetic field vanishes).

Remark 1.17. Classical mechanics and geometrical optics, discussed in this chapter, are intimately related. The configuration trajectories of mechanical systems are extremals of a variational principle, similar to the trajectories of light. In fact, mechanics can be described as a kind of geometrical optics; this was Hamilton's approach to mechanics (see [**3**] for details). The brachistochrone problem is a good example of this optics-mechanics analogy.

[3]Equivalently, one may consider billiards subject to the action of Coriolis force related to rotation of the Earth.

Chapter 4

Billiards inside Conics and Quadrics

The material in this chapter spans about 2,000 years: optical properties of conics were already known to ancient Greeks, whereas complete integrability of the geodesic flow on the ellipsoid is a discovery of 19-th century mathematics (Jacobi for a three-axial ellipsoid).

Recall the geometric definition of an ellipse: it is the locus of points whose sum of distances to two given points is fixed; these two points are called the foci. An ellipse can be constructed using a string whose ends are fixed at the foci – the method that carpenters and gardeners actually use; see figure 4.1. A hyperbola is defined similarly with the sum of distances replaced by the absolute value of their difference, and a parabola is the set of points at equal distances from a given point (the focus) and a given line (the directrix). Ellipses, hyperbolas and parabolas all have second order equations in Cartesian coordinates.

Exercise 4.1. Consider the ellipse with foci at points $(-c, 0)$ and $(c, 0)$ and the length of the string $2L$. Show that its equation is

$$\frac{x_1^2}{L^2} + \frac{x_2^2}{L^2 - c^2} = 1. \tag{4.1}$$

An immediate consequence is the following optical property of conics.

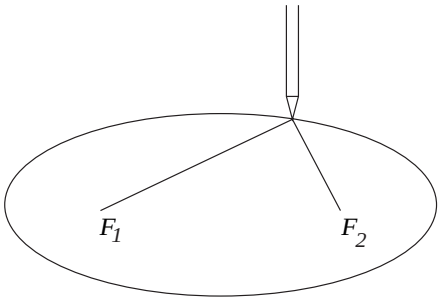

Figure 4.1. Gardener's construction of an ellipse

Lemma 4.2. *A ray of light through a focus of an ellipse reflects to a ray that passes through the other focus. A ray of light through a focus of a parabola reflects to a ray parallel to the axis of the parabola.*

We leave it to the reader to formulate a similar optical property of hyperbolas.

Proof. The ellipse in figure 4.1 is a level curve of the function $f(X) = |XF_1| + |XF_2|$; therefore the gradient of f is orthogonal to the ellipse. As in Chapter 1, $\nabla f(X)$ is the sum of two unit vectors in the directions F_1X and F_2X. It follows that the segments F_1X and F_2X make equal angles with the ellipse.

The argument for a parabola is similar, and we leave it to the reader. □

Exercise 4.3. Prove that the billiard trajectory through the foci of an ellipse converges to its major axis.

Here is an application of optical properties of conics: a construction of a trap for a beam of light, that is, a reflecting curve such that parallel rays of light, shone into it, get permanently trapped. There are a number of such constructions; the one in figure 4.2 is given by Peirone [**81**].

The curve γ is a part of an ellipse with foci F_1 and F_2; the curve Γ is a parabola with focus F_2. These curves are joined in a smooth way to produce a trap: it follows from Lemma 4.2 and Exercise 4.3

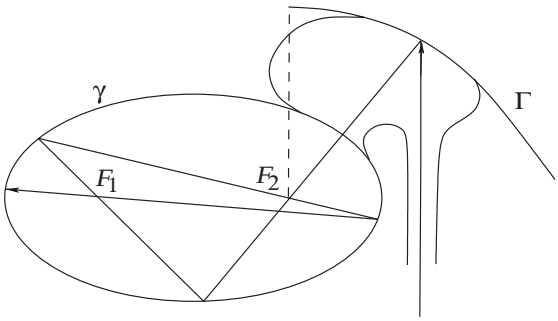

Figure 4.2. Trap for a beam of light

that a vertical ray, entering the curve through a window, will tend to the major axis of the ellipse and will therefore never escape.

The next question foreshadows Chapter 7: can one construct a compact trap for the set of rays sufficiently close to a given ray, that is, making small angles with it? See Digression 7.1 for the answer.

The construction of an ellipse with given foci has a parameter, the length of the string. The family of conics with fixed foci is called *confocal*. The equation of a confocal family, including ellipses and hyperbolas, is

$$\frac{x_1^2}{a_1^2+\lambda}+\frac{x_2^2}{a_2^2+\lambda}=1 \tag{4.2}$$

where λ is a parameter; compare to (4.1), in which the difference of the denominators is also constant.

Fix F_1 and F_2. Given a generic point X in the plane, there exist a unique ellipse and a unique hyperbola with foci F_1, F_2 through X; see figure 4.3. The ellipse and the hyperbola are orthogonal to each other: this follows from the fact that the sum of two unit vectors is perpendicular to its difference; cf. proof of Lemma 4.2. The two respective values of λ in equation (4.2) are called the *elliptic coordinates* of point X.

The next theorem says that the billiard ball map T in an ellipse is *integrable*. This means that there is a smooth function on the phase space, called an integral, which is invariant under T. We will describe

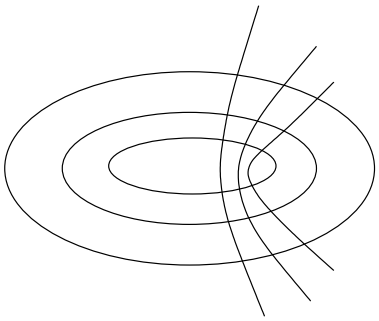

Figure 4.3. Elliptic coordinates in the plane

this property in two ways: geometrically and analytically. Consider an ellipse

$$\frac{x_1^2}{a_1^2} + \frac{x_2^2}{a_2^2} = 1$$

with foci F_1 and F_2. The phase space of the billiard ball map consists of unit vectors (x, v) with foot point on the ellipse and v having inward direction.

Theorem 4.4. *1) A billiard trajectory inside an ellipse forever remains tangent to a fixed confocal conic. More precisely, if a segment of a billiard trajectory does not intersect the segment F_1F_2, then all the segments of this trajectory do not intersect F_1F_2 and are all tangent to the same ellipse with foci F_1 and F_2; and if a segment of a trajectory intersects F_1F_2, then all the segments of this trajectory intersect F_1F_2 and are all tangent to the same hyperbola with foci F_1 and F_2.*

2) The function

$$\frac{x_1v_1}{a_1^2} + \frac{x_2v_2}{a_2^2} \tag{4.3}$$

is an integral of the billiard ball map.

Proof. We give an elementary geometry proof of 1). Let A_0A_1 and A_1A_2 be consecutive segments of a billiard trajectory. Assume that A_0A_1 does not intersect the segment F_1F_2; the other case is dealt

with similarly. It follows from the optical property, Lemma 4.2, that the angles $A_0A_1F_1$ and $A_2A_1F_2$ are equal; see figure 4.4.

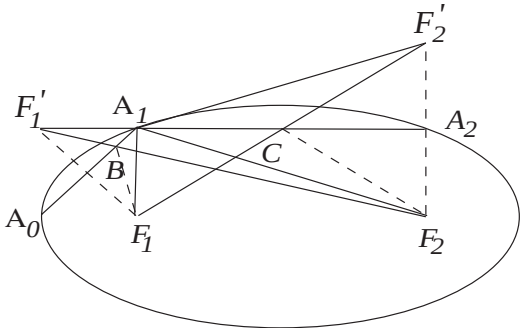

Figure 4.4. Integrability of the billiard in an ellipse

Reflect F_1 in A_0A_1 to F_1', and F_2 in A_1A_2 to F_2', and set: $B = F_1'F_2 \cap A_0A_1, C = F_2'F_1 \cap A_1A_2$. Consider the ellipse with foci F_1 and F_2 that is tangent to A_0A_1. Since the angles F_2BA_1 and F_1BA_0 are equal, this ellipse touches A_0A_1 at the point B. Likewise an ellipse with foci F_1 and F_2 touches A_1A_2 at the point C. One wants to show that these two ellipses coincide or, equivalently, that $F_1B + BF_2 = F_1C + CF_2$, which boils down to $F_1'F_2 = F_1F_2'$.

Note that the triangles $F_1'A_1F_2$ and $F_1A_1F_2'$ are congruent; indeed, $F_1'A_1 = F_1A_1, F_2A_1 = F_2'A_1$ by symmetry, and the angles $F_1'A_1F_2$ and $F_1A_1F_2'$ are equal. Hence $F_1'F_2 = F_1F_2'$, and the result follows.

To prove 2), let B be the diagonal matrix with entries $1/a_1^2$ and $1/a_2^2$. Then the ellipse can be written as $Bx \cdot x = 1$. Let (x, v) be a phase point and $(x', v') = T(x, v)$; see figure 4.5. We claim that $Bx \cdot v = Bx' \cdot v'$.

Start with the identity $B(x' + x) \cdot (x' - x) = 0$, which follows from the fact that x and x' belong to the ellipse and B is symmetric. Since v is collinear with $x' - x$, one has: $Bx \cdot v = -Bx' \cdot v$.

Next, consider the reflection at point x'. The vector Bx' is the gradient of the function $(Bx' \cdot x')/2$ and hence orthogonal to the

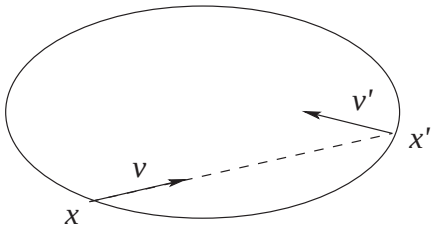

Figure 4.5. Billiard ball map

ellipse. The vector $v' + v$ is tangent to the ellipse; hence $Bx' \cdot v = -Bx' \cdot v'$. It follows that $Bx \cdot v = Bx' \cdot v'$. □

Of course, one could prove equivalence of the two statements of Theorem 4.4 directly; we do not dwell on this.

A *caustic*[1] of a plane billiard is a curve such that if a trajectory is tangent to it, then it remains tangent to it after every reflection. The caustics of the billiard in an ellipse are confocal ellipses and hyperbolas.

The phase portrait of the billiard in an ellipse is shown in figure 4.6. The phase space is foliated by invariant curves of the billiard ball map T. Each curve represents the family of rays tangent to a fixed confocal conic; these T-invariant curves correspond to the caustics. The ∞-shaped curve corresponds to the family of rays through the foci. The two singular points of this curve represent the major axis with two opposite orientations, a 2-periodic billiard trajectory. Another 2-periodic trajectory is the minor axis represented by two centers of the regions inside the ∞-shaped curve. Note how much simpler the phase portrait of the billiard in a circle is.

Let us mention that billiards bounded by confocal conics are integrable as well. An example is the annulus between two confocal ellipses.

Let us apply Theorem 4.4 to the illumination problem. Consider a plane domain with reflecting boundary: is it possible to illuminate it with a point source of light that emits rays in all directions?

[1] Burning, in Greek.

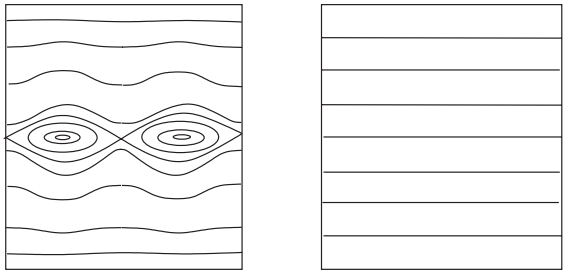

Figure 4.6. Phase portrait of the billiard in an ellipse and a circle

An example of a room that cannot be illuminated from any of its points is shown in figure 4.7;[2] the construction is due to L. and R. Penrose. The upper and lower curves are half-ellipses with foci F_1, F_2 and G_1, G_2. Since a ray passing between the foci reflects back again between the foci, no ray can enter the four "ear lobes" from the area between the lines F_1F_2 and G_1G_2, and vice versa. Thus if the source is above the line G_1G_2, the lower lobes are not illuminated; and if it is below F_1F_2, the same applies to the upper lobes.

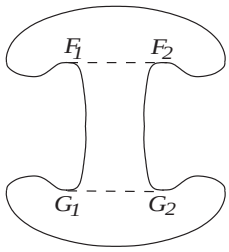

Figure 4.7. Illumination problem

Let us return to integrability of the billiard ball map T in an ellipse; see figure 4.6. The area preserving property of T implies that one can choose coordinates on the invariant curves in such a way that the map T is just a parallel translation: $x \mapsto x + c$. We now describe this important construction.

[2]Unlike geometrical optics, in wave optics any domain with smooth boundary is illuminated from every point.

Let M be a surface with an area form ω smoothly foliated by smooth curves. We will define an *affine structure* on the leaves of the foliation. This means that every leaf has a canonical coordinate system, defined up to an affine reparameterization $x \mapsto ax + b$.

Choose a function f whose level curves are the leaves of the foliation. Let γ be a curve $f = c$. Consider the curve γ_ε given by $f = c + \varepsilon$. Given an interval $I \subset \gamma$, consider the area $A(I, \varepsilon)$ between γ and γ_ε over I. Define the "length" of I as

$$\lim_{\varepsilon \to 0} \frac{A(I, \varepsilon)}{\varepsilon}.$$

Choosing a different function f, one multiplies the length of every segment by the same factor. Choose a coordinate x so that the length element is dx; this coordinate is well defined up to an affine transformation.

If the leaves of the foliation are closed curves, then one may assume that their lengths are unit. Then the coordinate x on every leaf varies on the circle $S^1 = \mathbf{R}/\mathbf{Z}$ and is defined up to a parallel translation $x \mapsto x + c$.

Suppose now that a smooth map $T : M \to M$ preserves the area ω and the foliation leaf-wise. Such a map is called integrable. Then T preserves the affine structure on the leaves and is itself given by a formula $T(x) = ax + b$. If the leaves are closed, then T is a parallel translation in the respective affine coordinate.

Corollary 4.5. *Let T be an integrable area preserving map of a surface, and assume that the invariant curves are closed. If an invariant curve γ contains a k-periodic point, then every point of γ is k-periodic.*

Proof. In an affine coordinate, $T(x) = x + c$. If $T^k(x) = x$, then $kc \in \mathbf{Z}$, and therefore $T^k = \mathrm{id}$. □

Assume that two maps, T_1 and T_2, preserve an area form and a foliation with closed leaves leaf-wise. Then T_1 and T_2 are parallel translations in the same affine coordinate system on each leaf. Since parallel translations commute, one has: $T_1 T_2 = T_2 T_1$. Applying this observation to billiards inside ellipses yields the next corollary.

Corollary 4.6. *Consider two confocal ellipses and let T_1, T_2 be the billiard ball maps defined on oriented lines that intersect both. Then the maps T_1 and T_2 commute.*

As a particular case, consider the rays through the foci. Lemma 4.6 implies the following "most elementary theorem of Euclidean geometry" by M. Urquhart:[3] $AB + BF = AD + DF$ if and only if $AC + CF = AE + EF$; see figure 4.8.

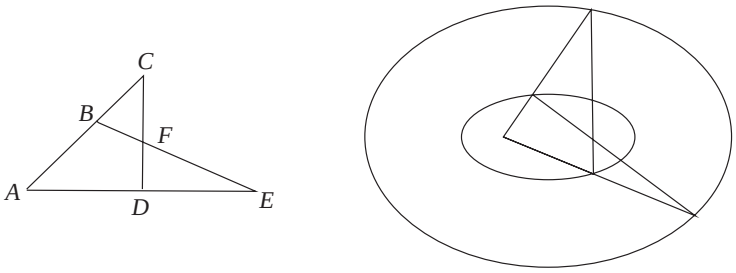

Figure 4.8. The most elementary theorem of Euclidean geometry

The reader is challenged to find an elementary proof of this theorem.

4.1. Digression. Poncelet porism. The integrability of the billiard ball map in an ellipse described in Theorem 4.4 has an interesting consequence.

Consider two confocal ellipses, $\gamma \subset \Gamma$. Pick a point $x \in \Gamma$ and draw a tangent line to γ. Consider the billiard trajectory whose first segment lies on this line. By Theorem 4.4, every segment of this trajectory is tangent to γ. Assume that this trajectory is n-periodic, that is, closes up after n steps. Now choose another starting point $x_1 \in \Gamma$ and repeat this construction. It follows from Corollary 4.5 that the respective billiard trajectory closes up after n steps as well. Indeed, the family of lines tangent to γ is an invariant curve of the billiard ball map in Γ.

[3]Discovered when considering fundamental concepts of the theory of special relativity.

In fact, the assumption that Γ and γ are confocal is not necessary at all for the conclusion of the closure theorem to hold. One has the following Poncelet theorem (a.k.a. Poncelet porism); see figure 4.9.

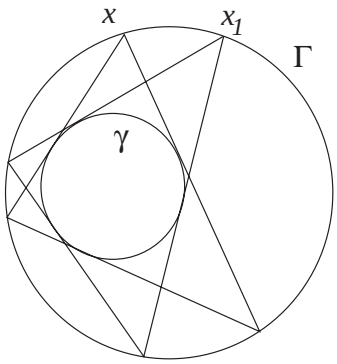

Figure 4.9. Poncelet closure theorem

Theorem 4.7. *Let $\gamma \subset \Gamma$ be two nested ellipses and let $x \in \gamma$ be a vertex of an n-gon inscribed in Γ and circumscribed about γ. Then every point $x_1 \in \Gamma$ is a vertex of such an n-gon.*

One way to prove this theorem is to show that any pair of nested ellipses can be obtained from confocal ones by a projective transformation of the plane; a projective transformation takes lines to lines, and a Poncelet configuration to another one. We will give a different, more direct, proof, and then, in Chapter 9, return to the Poncelet theorem again.

Proof. Choose an orientation of γ. Given $x \in \Gamma$, draw the oriented tangent line through x to γ and let y be its intersection point with Γ. One has a smooth map $T(x) = y$ from Γ to itself. We will construct a coordinate on Γ in which the map T is a parallel translation $t \mapsto t + c$.

Applying an affine transformation, assume that Γ is a circle. Let x be an arc length parameter on Γ. We are looking for a T-invariant length element (a differential 1-form) $f(x)\,dx$.

Denote by $R_\gamma(x)$ and $L_\gamma(x)$ the lengths of the positive (right) and negative (left) tangent segments from x to γ. Consider a point x_1, infinitesimally close to x. Let $O = xy \cap x_1y_1$ and ε the angle between xy and x_1y_1. Note that the line x_1y_1 makes equal angles with the circle Γ; denote this angle by α (see figure 4.10.)[4] By the Sine theorem,

$$\frac{|yy_1|}{L_\gamma(y)} = \frac{\sin\varepsilon}{\sin\alpha} = \frac{|xx_1|}{R_\gamma(x)}$$

or

$$\frac{dy}{L_\gamma(y)} = \frac{dx}{R_\gamma(x)}. \tag{4.4}$$

Assume for the moment that γ is a circle too. Then the right and left tangent segments are equal: $R_\gamma(x) = L_\gamma(x)$. Denote this common value by $D_\gamma(x)$. It follows from (4.4) that the 1-form $dx/D_\gamma(x)$ is T-invariant.

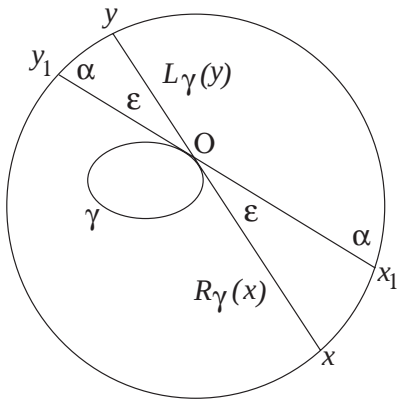

Figure 4.10. Proving the Poncelet theorem

Finally, if γ is not a circle, let A be an affine transformation that takes γ to one. We have:

$$\frac{R_\gamma(x)}{L_\gamma(y)} = \frac{R_{A\gamma}(Ax)}{L_{A\gamma}(Ay)} = \frac{D_{A\gamma}(Ax)}{D_{A\gamma}(Ay)}.$$

[4]What follows is, essentially, the argument from Theorem XXX, figure 102, in I. Newton's "Principia"; Newton studies the gravitational attraction of spherical bodies.

Setting $f(x) = 1/D_{A\gamma}(Ax)$, one obtains a T-invariant 1-form $f(x)\,dx$.

It remains to choose a coordinate t in which $f(x)\,dx = dt$. Then the map T becomes a translation $t \to t + c$, and Poncelet's theorem follows. □

Exercise 4.8. Let Γ and γ be circles of radii R and r, and let a be the distance between their centers.

a) Prove that one has a 3-periodic Poncelet configuration if and only if $a^2 = R^2 - 2rR$.

b)* Prove that one has a 4-periodic Poncelet configuration if and only if $(R^2 - a^2)^2 = 2r^2(R^2 + a^2)$.

Necessary and sufficient conditions, in terms of two conics, for a Poncelet polygon to close after n steps are due to Cayley; see [**12**].

Poncelet's theorem has numerous proofs and generalizations; see [**18**] for a thorough discussion. Poncelet discovered this result in 1813-14, when he was a prisoner of war in the Russian city of Saratov; he published his theorem in 1822, upon returning to France.

In conclusion of this digression, let us return to billiards in ellipses. Let $\Gamma_1, \Gamma_2, \dots, \Gamma_n$ be confocal ellipses and γ another confocal ellipse inside them all. Let T_i be the billiard map in Γ_i considered as a transformation of the space of oriented lines in the plane. Each T_i is integrable, and these maps share invariant curves that consist of the lines, tangent to confocal ellipses, such as γ. Hence we can choose an affine parameter t on this invariant curve so that each T_i is a parallel translation $t \mapsto t + c_i$. Therefore, in the construction of the Poncelet polygons, one could choose the first vertex on Γ_1, the second on Γ_2, etc., the n-th on Γ_n: the conclusion of the closure theorem would hold without change.[5] ♣

The rest of this chapter is devoted to two closely related results: complete integrability of the billiard ball map inside the ellipsoid and of the geodesic flow on the ellipsoid. As the first step toward this goal we discuss the notion of *polar duality*.

[5] An interesting addition to Poncelet's theorem was recently made by R. Schwartz; see [**92**].

Let V be a vector space and V^* its dual. Every non-zero vector $x \in V$ determines an affine hyperplane $H_x \subset V^*$ that consists of covectors p such that $p \cdot x = 1$ where the dot denotes the pairing between vectors and covectors. Likewise, a non-zero covector $p \in V^*$ determines a hyperplane $H_p \subset V$ consisting of $x \in V$ satisfying the same equation.

Exercise 4.9. Show that $x \in H_p$ if and only if $p \in H_x$.

Let $M \subset V$ be a smooth star-shaped hypersurface; this means that the position vector of every point $x \in M$ is transverse to M. The tangent plane at x is H_p for some $p \in V^*$. The set of these p is a hypersurface $M^* \subset V^*$ called polar dual to M. The next lemma justifies the terminology.

Lemma 4.10. *The hypersurface dual to M^* is M.*

Proof. Let v be a test tangent vector to M^* at point p. We want to show that $v \in H_x$. Since v is tangent to M^*, the covector $p + \varepsilon v$ is ε^2-close to M^*. Therefore, up to terms second order in ε, the covector $p + \varepsilon v$ is dual to a point of M, infinitesimally close to x. Ignoring terms of higher order in ε, write this point as $x + \varepsilon u$ where u is a tangent vector to M at x. Thus one has

$$(p + \varepsilon v) \cdot (x + \varepsilon u) = 1$$

and hence

$$v \cdot x + p \cdot u = 0.$$

Since $u \in H_p$, one has $p \cdot u = 0$. Hence $v \cdot x = 0$, and therefore $v \in H_x$. □

The following example will be important for us.

Example 4.11. Let V be Euclidean space, A a self-adjoint linear operator and M the quadric $Ax \cdot x = 1$. The gradient of the quadratic function $Ax \cdot x$ at point x is $2Ax$; therefore the tangent hyperplane to M at x is orthogonal to Ax. It follows that $T_x M = H_p$ with $p = Ax$. The dual hypersurface M^* is given by $A^{-1}p \cdot p = 1$; in particular, M^* is also a quadric.

Consider an ellipsoid M in $\mathbf{R}^n$ given by the equation

$$\frac{x_1^2}{a_1^2} + \frac{x_2^2}{a_2^2} + \cdots + \frac{x_n^2}{a_n^2} = 1, \tag{4.5}$$

and assume that all semiaxes $a_1, \ldots, a_n$ are distinct. Let B be the diagonal matrix with entries $1/a_1^2, \ldots, 1/a_n^2$, and set $A = B^{-1}$. The equation of M is $Bx \cdot x = 1$. We define the confocal family of quadrics M_λ by the equation

$$\frac{x_1^2}{a_1^2 + \lambda} + \frac{x_2^2}{a_2^2 + \lambda} + \cdots + \frac{x_n^2}{a_n^2 + \lambda} = 1 \tag{4.6}$$

where λ is a real parameter. The topological type of M_λ changes as λ passes the values $-a_i^2$. A shorthand formula for the confocal family is

$$(A + \lambda E)^{-1} x \cdot x = 1,$$

where E is the unit matrix.

The next theorem by Jacobi extends the elliptic coordinates from the plane to n-dimensional space.

Theorem 4.12. *A generic point $x \in \mathbf{R}^n$ is contained in exactly n quadrics confocal with the given ellipsoid. These confocal quadrics are pairwise perpendicular at x.*

Proof. We give two proofs, the first based on the notions of polar duality and an eigenbasis of a quadratic form. The second one is much more straightforward.

1) A quadric M_λ passes through x if and only if the hyperplane H_x is tangent to the dual quadric M_λ^*. Thus we want to show that H_x is tangent to n quadric from the dual family M_λ^*.

According to Example 4.11, M_λ^* is given by equation $(A + \lambda E)p \cdot p = 1$. A normal vector to this hypersurface at point p is $(A + \lambda E)p$, and a normal vector to the hyperplane H_x is x. Thus we are looking for λ and p such that

$$(A + \lambda E)p \cdot p = 1, \quad (A + \lambda E)p = \mu x. \tag{4.7}$$

Consider the quadratic form $(1/2)(Ap \cdot p - (p \cdot x)^2)$. This quadratic form has an eigenbasis $p_1, \ldots, p_n$ with the eigenvalues $-\lambda_1, \ldots, -\lambda_n$

such that $Ap_i - (p_i \cdot x)x = -\lambda_i p_i$. Hence

$$(A + \lambda_i E)p_i = (p_i \cdot x)x. \tag{4.8}$$

Rescale p_i so that $p_i \cdot x = 1$. Then (4.8) implies:

$$(A + \lambda_i E)p_i \cdot p_i = x \cdot p_i = 1,$$

and conditions (4.7) are satisfied.

Finally, the eigenvectors $p_1, \dots, p_n$ are orthogonal, and so are the hyperplanes $H_{p_1}, \dots, H_{p_n}$ tangent to the quadrics $M_{\lambda_1}, \dots, M_{\lambda_n}$.

2) Consider equation (4.6), and assume that $a_1^2 < \cdots < a_n^2$. Given an x, we want to find λ satisfying this equation. This reduces to a polynomial in λ of degree n, and one wants to show that all its roots are real.

Consider the segment between a_i^2 and a_{i+1}^2. The left-hand side F of (4.6) assumes the values $-\infty$ and ∞ at the end point of this interval; hence it also assumes the value 1. There are $n-1$ such intervals, and in addition, F varies from ∞ to 0 on the infinite interval (a_n^2, ∞). Hence the equation $F = 1$ has n roots $\lambda_1, \dots, \lambda_n$, distinct for a generic x.

Now we need to prove that the quadrics M_{λ_i} and M_{λ_j} are orthogonal at point x. As in Example 4.11, consider the normal to M_{λ_i}

$$n_i = \left(\frac{x_1}{a_1^2 + \lambda_i}, \frac{x_2}{a_2^2 + \lambda_i}, \dots, \frac{x_n}{a_n^2 + \lambda_i} \right).$$

Then

$$n_i \cdot n_j = \frac{x_1^2}{(a_1^2 + \lambda_i)(a_1^2 + \lambda_j)} + \cdots + \frac{x_n^2}{(a_n^2 + \lambda_i)(a_n^2 + \lambda_j)}. \tag{4.9}$$

Consider equations (4.6) for λ_i and λ_j. The difference of their left-hand sides is equal to the right-hand side of (4.9) times $(\lambda_j - \lambda_i)$, and this right-hand side is zero. Therefore $n_i \cdot n_j = 0$, as claimed. □

The next theorem is due to Chasles.

Theorem 4.13. *A generic line in* $\mathbf{R}^n$ *is tangent to* $(n-1)$ *distinct quadrics from a given confocal family. The tangent hyperplanes to these quadrics at the points of tangency with the line are pairwise orthogonal.*

Proof. Project $\mathbf{R}^n$ along the given line onto its $(n-1)$-dimensional orthogonal complement. A quadric determines a hypersurface in this $(n-1)$-dimensional space, the set of critical values of its projection (the apparent contour). If one knows that these hypersurfaces also constitute a confocal family of quadrics, the statement will follow from Theorem 4.12.

It is not hard to prove that the apparent contour of a quadric is a quadric by a direct computation (see Exercise 4.14 below). However the computation becomes quite involved when proving that the apparent contours of confocal quadrics are also confocal quadrics. We will proceed as in the first proof of the preceding theorem and make full use of polar duality.

Let v be the direction vector of the projection, and let $M \subset V$ be a smooth star-shaped hypersurface. Let $W \subset V^*$ be the hyperplane consisting of those covectors p that vanish on v. Suppose that a line parallel to v is tangent to M at point x. Then the tangent hyperplane T_xM contains v. This tangent hyperplane is H_p for some $p \in V^*$. Hence $p \cdot v = 0$, and therefore $p \in W$. We conclude that polar duality takes the points of tangency of M with the lines, parallel to v, to the intersection of the dual hypersurface M^* with the hyperplane W; see figure 4.11.

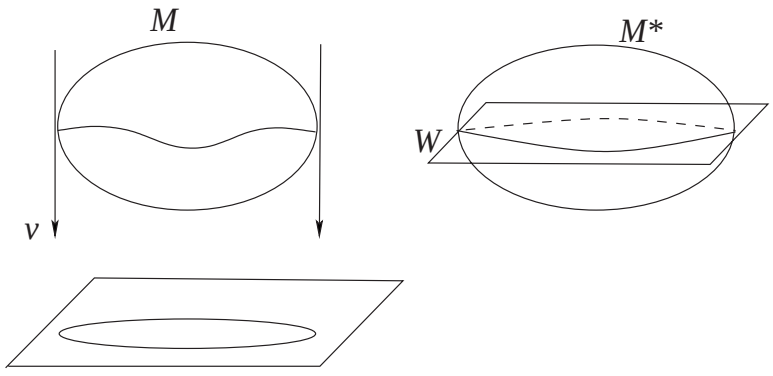

Figure 4.11. Duality between projection and intersection

On the other hand, the hyperplane W is the dual space to the quotient space V/v (identified with the orthogonal complement to v). Therefore the apparent contour of M in this quotient space is polar dual to $M^* \cap W$. Recall Example 4.11: if M belongs to a confocal family $(A+\lambda E)^{-1}x \cdot x = 1$, then M^* belongs to the family $(A+\lambda E)p \cdot p = 1$. The intersection of the latter with a hyperplane is a family of the same type, and therefore its polar dual is a confocal family. This proves that the apparent contours of confocal quadrics are also confocal quadrics. □

Exercise 4.14. Show, by a direct computation, that the apparent contour of a quadric $Ax \cdot x = 1$ is a quadric.

Hint: The line $y + tv$ is tangent to the quadric if and only if the quadratic equation

$$A(y+tv) \cdot (y+tv) = 1$$

has a multiple root in t. What is the discriminant of this equation?

Let M be a hypersurface in $\mathbf{R}^n$. A *geodesic curve* on M is a curve that locally minimizes the distance between its points. In other words, a geodesic is a trajectory of light in M or a trajectory of a free point confined to M. If $\gamma(t)$ is an arc length parameterized geodesic, then the acceleration vector $\gamma''(t)$ is orthogonal to M (physically, this means that the only force acting on the point is the normal force that confines the point to M). For example, a geodesic on the unit sphere is its great circle. The motion of a free point is described by the geodesic flow on the tangent bundle TM: given a vector (x, v), the foot point x moves with the constant speed $|v|$ along the geodesic in the direction v and the velocity remains tangent to this geodesic.

The geodesic flow on the ellipsoid $M \subset \mathbf{R}^n$ is completely integrable: it has $n-1$ invariant functions. One of them is the energy $|v|^2/2$, and the other $n-2$ are described geometrically in the following theorem.

Theorem 4.15. *The tangent lines to a fixed geodesic on M are tangent to $(n-2)$ other fixed quadrics confocal with M.*

Proof. Let ℓ be a tangent line to M at point x. By Theorem 4.13, ℓ is tangent to $(n-2)$ confocal quadrics $N_1, \dots, N_{n-2}$. Consider

an infinitesimal rotation of ℓ along the geodesic on M through x in the direction of ℓ. Modulo infinitesimals of the second order, ℓ rotates in the 2-plane generated by ℓ and the normal vector n to M at x. By Theorem 4.13, the tangent hyperplane to the quadric N_i, $i = 1, \dots, n-2$, at the point of its tangency with ℓ contains n. Hence, modulo infinitesimals of the second order, the line ℓ remains tangent to N_i, and the claim follows. □

As an application, consider an ellipsoid $M^2 \subset \mathbf{R}^3$. The lines tangent to a fixed geodesic γ on M are tangent to another quadric N confocal with M. Let x be a point of M. The tangent plane to M at x intersects N along a conic. The number of tangent lines to this conic from x can be equal to 2, 1 or 0 (the intermediate case of a single tangent line, having multiplicity 2, happens when x belongs to the conic). Thus the surface M gets partitioned into two parts depending on the number, 2 or 0, of common tangent lines of M and N. The geodesic γ is confined to the former part and can have only one of the two possible directions in every point; see figure 4.12.

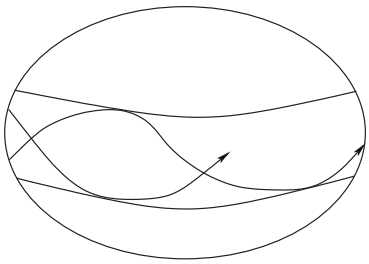

Figure 4.12. A geodesic on the ellipsoid

If one lets $a_n \to 0$ in (4.5), then the quadratic hypersurface $M^{n-1} \subset \mathbf{R}^n$ degenerates to a doubly covered ellipsoid $D^{n-1} \subset \mathbf{R}^{n-1}$. The geodesic lines on M become billiard trajectories in D. As a consequence, the billiard ball map inside an $(n-1)$-dimensional ellipsoid is also completely integrable: a billiard trajectory remains tangent to $n-2$ confocal quadrics. In the plane case, this is familiar from Theorem 4.4.

Explicit formulas for the integrals of the billiard ball map in an n-dimensional ellipsoid are as follows (cf. Theorem 4.4 for the plane case). Let the ellipsoid be bounded by the hypersurface (4.5). Let (x, v) be a phase point, a unit inward tangent vector whose foot point x lies on the boundary. The following functions are invariant under the billiard ball map:

$$F_i\ (x, v) = v_i^2 + \sum_{j \neq i} \frac{(v_i x_j - v_j x_i)^2}{a_j^2 - a_i^2}, \quad i = 1, \dots, n.$$

These functions are not independent: $F_1 + \dots + F_n = 1$.

Let us add that the billiard ball map inside quadratic hypersurfaces is completely integrable in the spherical and hyperbolic geometries as well. One considers the unit (pseudo)sphere described in Digression 3.1 and intersects it with a quadratic cone given by an equation $Ax \cdot x = 0$. The intersection is, by definition, a quadratic hypersurface in the respective geometry.

For various approaches to complete integrability of the geodesic flow on the ellipsoid and the billiard system inside the ellipsoid, see [**73, 72, 74, 112**].

4.2. Digression. Complete integrability, Arnold-Liouville theorem. Recall that integrability of the billiard ball map inside an ellipse implies strong restrictions on the behavior of the map: for example, if an invariant curve contains an n-periodic point, then all points are n-periodic. This follows from the area preserving property of the billiard ball map.

Likewise, complete integrability of a symplectic map, such as the billiard ball map, in multi-dimensional cases imposes severe restrictions on its dynamics. To formulate the relevant theorem, we need to make another excursion to symplectic geometry; see [**3, 7, 67**].

Let (M, ω) be a symplectic manifold. The symplectic structure identifies tangent and cotangent vectors: a vector u determines a linear function $v \mapsto \omega(u, v)$. Let f be a smooth function on M. The differential df is a 1-form which therefore corresponds to a vector field X_f. This field is called a *Hamiltonian vector field* and the function f a *Hamiltonian function*. This resembles a more familiar construction of

the gradient of a function f which is a vector field associated with df by a Euclidean structure (or, more generally, a Riemannian metric), and X_f is sometimes called the symplectic gradient of f.

One can define a binary operation on smooth functions on a symplectic manifold called the *Poisson bracket* and denoted by $\{f, g\}$. The Poisson bracket of two functions is the directional derivative of one of them along the Hamiltonian vector field of the other:

$$\{f, g\} = df(X_g) = \omega(X_f, X_g).$$

Two functions f and g are said to Poisson commute if $\{f, g\} = 0$.

The Poisson bracket satisfies two remarkable identities:

$$\{f, g\} = -\{g, f\}, \quad \{f, \{g, h\}\} + \{g, \{h, f\}\} + \{h, \{f, g\}\} = 0. \tag{4.10}$$

This means that smooth functions on a symplectic manifold constitute a *Lie algebra*.

Exercise 4.16. Let $\omega = dp \wedge dq$ and $f(q, p),\ g(q, p),\ h(q, p)$ be smooth functions.

a) Find the formula for X_f.

b) Find the formula for $\{f, g\}$.

c) Check identities (4.10).

There are different definitions of complete integrability; the one we consider is called integrability in the sense of Liouville. A symplectic map $T : M^{2n} \to M^{2n}$ is called completely integrable if there exist T-invariant Poisson commuting smooth functions $f_1, \dots, f_n$ (integrals). We assume that these functions are independent almost everywhere on M; that is, their differentials (or symplectic gradients) are linearly independent at almost every point.

Generic level sets of the functions $f_1, \dots, f_n$ are n-dimensional Lagrangian submanifolds that foliate M. Similarly to the 2-dimensional case, each of these submanifolds has an affine structure. In this affine structure, the map T is an affine transformation. If such a level manifold is connected and compact, then it is an n-dimensional torus, and T is a parallel translation. The statements in this paragraph constitute the Arnold-Liouville theorem.

We discussed torus parallel translations in Chapter 2. In particular, if a translation has a periodic point, then all points are periodic with the same period.

The billiard ball map inside an ellipsoid in $\mathbf{R}^n$ is completely integrable. The phase space is a $2(n-1)$-dimensional symplectic manifold, and the map has $n-1$ integrals, one for each confocal quadric to which a billiard trajectory remains tangent. These integrals Poisson commute, the fact that we did not prove.

Everything we said about discrete time systems (symplectic maps) holds for continuous time systems (Hamiltonian vector fields). An important example of a Hamiltonian vector field is the geodesic flow on a Riemannian manifold M. The phase space of this flow is T^*M (identified with TM via the metric) with its standard symplectic structure, and the Hamiltonian function is the energy $|p|^2/2$. The geodesic flow on an ellipsoid is completely integrable in the sense of Liouville. ♣